NSG-7645

Research Report R82-1

MIT

FINITE ELEMENT ANALYSIS OF NONISOTHERMAL POLYMER PROCESSING OPERATIONS

by
Craig Douglas
and
David Roylance

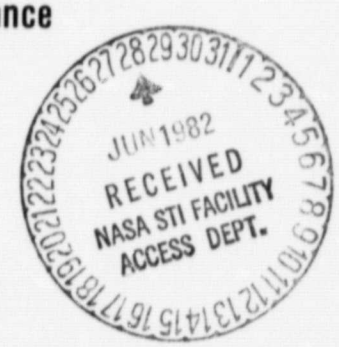

April 1982

DEPARTMENT
OF
MATERIALS SCIENCE
AND
ENGINEERING

SCHOOL OF ENGINEERING
MASSACHUSETTS INSTITUTE OF TECHNOLOGY
Cambridge, Massachusetts 02139

FINITE ELEMENT ANALYSIS OF NONISOTHERMAL POLYMER PROCESSING OPERATIONS

Craig Douglas and David Roylance

Department of Materials Science and Engineering
Massachusetts Institute of Technology
Cambridge, Massachusetts 02139 USA

INTRODUCTION

Finite element analysis offers great promise for reducing the empiricism now used extensively in polymer processing design, since it is well suited for modeling the complicated boundary conditions and material properties encountered in industrial practice. This paper will present the formulation we have developed for use in such processing analyses, and results which illustrate its use in some typical situations. Our element formulations are constructed on the premise that momentum convection can be neglected (polymer melt flows typically have very low Reynolds' numbers), but that convective heat transfer may be significant (high Peclet numbers). Nonisothermal effects are considered important in polymer processing, due in part to the significant heating which may occur due to viscous dissipation, and also to the very strong influence of temperature on fluid viscosity. This paper will not discuss problems in which the temperature dependence of viscosity is considered,

although our code does have the capability for such problems. Here we will treat the flow as Newtonian, with the flow field being coupled to the heat transfer equation only through the viscous heat generation.

MODEL FORMULATION

Governing Equations.

The velocity and temperature fields are governed by the conservation equations for momentum and energy as shown below (a list of nomenclature appears at the end of the paper):

$$\rho\,(Du/Dt) = -\nabla p + \mu\nabla^2 u$$

$$\rho\, c(DT/Dt) = k\nabla^2 T + Q$$

In our work the velocity field is constrained to be incompressible ($\nabla u = 0$) and the heat generation Q is given by the viscous dissipation ($Q = \tau:\nabla u$). Boundary conditions on velocity, stress, temperature and heat flux are also present on various portions of the boundary, and the ease with which these conditions are handled by the finite element procedure constitutes one of its most attractive features.

Finite Element Equations.

As is described in detail in several texts (e.g. ref. 1), the finite element equations may be developed from the governing equations and their boundary conditions by recasting the equations in a Galerkin weighted residual formulation, applying Green's Theorem to lower the order of second derivatives and introduce natural boundary conditions, and finally by expressing the problem variables in terms of an interpolation among their values at various nodes which are located at finite elements within the problem domain.

In our formulation the nodal unknowns are taken as the velocity components and the temperature, so that:

$$(u,T) = N_i a_i$$

where the i subscript refers to nodal values and the N functions are interpolation polynomials computed by standardized subroutines for isoparametric elements. The finite element equations can be written in the form:

$$C\dot{a} + Ka = f$$

where

$$C = \begin{bmatrix} C^{\rho} & 0 \\ 0 & C^{T} \end{bmatrix}, \quad K = \begin{bmatrix} K^{\lambda} + K^{\mu} & 0 \\ 0 & K^{T} + K^{c} + K^{h} \end{bmatrix}, \quad f = \begin{Bmatrix} f^{t} \\ f^{T} + f^{h} \end{Bmatrix}$$

The components in these global matrices are assembled from corresponding element submatrices given in the following list:

$$c^{\rho} = \int_{\Omega} N\ N\, d\Omega \qquad \text{(fluid inertia)}$$

$$c^{T} = \int_{\Omega} \bar{N} \rho c N\, d\Omega \qquad \text{(thermal inertia)}$$

$$k^{\lambda} = \int_{\Omega} (m^{T}B)^{T} \lambda (m^{T}B)\, d\Omega \qquad \text{(compressibility penalty)}$$

$$k^{\mu} = \int_{\Omega} B^{T} D B\, d\Omega \qquad \text{(viscosity)}$$

$$k^{T} = \int_{\Omega} (\nabla^{T} N) k \nabla N\, d\Omega \qquad \text{(thermal conduction)}$$

$$k^c = \int_\Omega N \rho c \, u^T \nabla N \, d\Omega \qquad \text{(thermal convection)}$$

$$k^h = \int_{\Gamma^h} NhN \, d\Gamma \qquad \text{(boundary convection)}$$

$$f^t = -\int_{\Gamma^t} Nt^* \, d\Gamma \qquad \text{(applied tractions)}$$

$$\underline{f} = \int_\Omega N\underline{Q} \, d\Omega \qquad \text{(heat generation)}$$

$$f = -\int_{\Gamma^h} NhT_a \, d\Gamma \qquad \text{(ambient temperature)}$$

We have chosen to compute various time-step values for transient problems using the "theta method" described in Reference 1. This algorithm may be written as:

$$[(C/\Delta t) + \theta K]a_{n+1} + [(-C/\Delta t) - (1-\theta)K]a_n = (1-\theta)f_n + \theta f_{n+1}$$

Here the n and n+1 subscripts refer to values at the current and next time, and θ is a parameter between zero and one which determines the weight to be given the next time step. The algorithm is unconditionally stable for $\theta > .5$, and $\theta = .667$ corresponds to a Galerkin treatment with a linear interpolation over the time increment.

All of this formulation is conventional, and a more detailed discussion of its underlying theory and computer implementation can be found elsewhere [1,2]. Some specific items might be mentioned here, however: (1) A penalty formulation is used to enforce incompressibility, rather than the usual velocity-pressure approach. This requires the use of double-precision computer arithmetic and a selectively reduced order of numerical integration for sufficient accuracy, but offers some reduction in programming effort and eliminates the need to compute pressure as an additional nodal variable. (2) The formulation assumes a full coupling between the viscous and thermal terms, with the resulting storage and manipulation of zeroes as seen in the above matrix equations. This coupling is unnecessary and inefficient for the partially coupled example problems described below, in which the flow field could be solved separately and then used in a single heat transfer solution. However, the coupled formulation is more general and we expect the majority of our work will require it. (3) We have coded a capability for either conventional Galerkin or "optimal" upwinding for the handling of the thermal convection term. The upwinding formulation is very conven-

ient, as it requires simply a one-point evaluation at a suitably shifted Gauss point within each element [2], but this approach is controversial and evidence can be cited as to its failure in some instances [3].

EXAMPLE PROBLEMS

Entry Flow.

Figure 1 shows the streamlines for a 4:1 entry flow which we have previously reported in greater detail [4]. Here a grid of 100 four-node linear elements were used to model the upper symmetric half of the plane capillary , and a fully-developed Poiseuille velocity distribution was imposed at the reservoir entry as a boundary condition. The streamlines are identical with published experimental and numerical results, although the grid used here was not intended to be fine enough to capture the weak recirculation which develops in the stagnant corner of the reservoir.

The temperature contours for convectionless flow are shown in Figure 2, which shows a hot region at the entrance of the capillary due to the combination of higher viscous dissipation at this region and a greater distance from cooi boundaries to which heat may be conducted. These isotherms are normalized on the maximum centerline temperature $T = \mu V^2/3k$ expected for Poiseuille flow in the capillary.

The importance of thermal convection in this problem is given approximately by the Peclet number $Pe = UL\rho c/k$, where we may take U to be the maximum (centerline) velocity in the capillary and L as the capillary half-height. Figure 3 plots the variation of temperature along the centerline for various values of Pe, and it can be seen that the effect of increased thermal convection is to sweep the cooler upstream flow particles well into the capillary, with a resulting lowering of the temperatures overall and a shift downstream of the hot spot near the throat. The relatively coarse grid used in this problem produced unstable Galerkin results for Peclet numbers greater than approximately ten, and so the higher degrees of thermal convection were computed using the upwinding formulation. Further tests with refined grids should be completed to assess the accuracy of the upwinded solutions, although the plots in Figure 3 appear reasonable.

Transient Couette Flow.

We have found that a capability for dynamic solutions is very useful not only in explicitly transient problems, but for a variety of processing flows. Rather than discretizing the entire bubble in a film blowing process, for instance, we follow a small annular strip dynamically as it travels from the die to the frost line. The dynamic algorithm is also useful for developing steady solutions to nonlinear problems, and we are presently working at modeling the flow of reactive fluids in this manner.

The performance of the time-stepping algorithm will be illustrated here by means of some one-dimensional problems in which a single row of linear elements is used. Figure 4 shows such a strip which is used to model a Couette flow in which the upper plate is set into motion impulsively, and in which the velocity gradients in the horizontal direction are zero. It is necessary in such problems to consider both the mesh spacing and the time step carefully, in order that both are able to capture sharp gradients which occur near the moving wall. It is noted that the mesh becomes much more refined near the upper plate in order to capture the boundary layer which develops there. We have also used a time step which begins very small and then increases logarithmically as the flow develops. The velocity histories at three positions in the flow field are plotted in figure 4 and compared with the theoretical solution. It is clear that the computed solutions are not exact, but that the correct steady values are obtained at long times; improvement in accuracy could likely be obtained by considering further refinements in the mesh and the choice of time steps.

Figure 5 shows the velocity and temperature profiles for a similar problem, different only in that here the upper 15% of the fluid is a layer having a viscosity ten times that of the remaining 85%. This simulation is aimed at modeling the flow which may occur in coextrusion. At early times, the flow has not developed sufficiently to involve the low-viscosity fluid away from the upper plate. The thermal dissipation in the upper region is initially intense due to

the very high shear rates in the boundary layer, and a severe thermal spike develops. At longer times the flow is fully developed through the low-viscosity fluid; the high-viscosity region experiences only little shear flow and appears almost as a rigid boundary. The temperature profile in the low-viscosity fluid then becomes parabolic as expected in simple Couette flow.

Graetz Flow.

The Graetz or forced convection problem is a commonly used trial problem in which channel flow suddenly encounters a heated portion of the boundary. In the absence of flow the temperature distribution is based only on conductive heat transfer considerations, but with significant flow the cooler upstream particles are swept downstream; a thermal boundary layer develops at the heated boundary which grows gradually toward the channel center and the contours of constant temperature are swept downstream relative to the conduction-only case.

Figure 6 shows the isotherms for Peclet Numbers of 1.3 and 130, where upwinding was used to compute the high-convection case. The boundary conditions included an imposed pressure at the entrance of the channel, and the heated boundary was located a sufficient distance from the entry to permit the development of a Poiseuille flow. In this example the viscous generation of heat was assumed negligible, so heat is added only at the boundary.

CONCLUSIONS

This paper has described some features of a model which is being developed in our laboratory to simulate a number of diverse polymer melt processing operations. We hope that this inexpensive and easily implemented model can provide a means by which the designer's intuition might be expanded. Continuing work is aimed at increasing the number of process situations amenable to this type of modeling; among these are included reactive flows, free surfaces, and wall slip.

NOMENCLATURE

B	Matrix of interpolation function derivatives
c	specific heat
D	Fluid viscosity matrix
D/D_t	Substantive derivative
h	Coefficient of convective boundary heat transfer
k	Coefficient of thermal conduction
L	Characteristic length
m	Identity vector (1,1,1,0,0,0)
n	Unit normal vector
N	Interpolation function
p	Pressure
T	Temperature
T_a	Ambient temperature

u	Velocity vector
V	Rate of deformation tensor
Γ^h	Boundary on which thermal convection occurs
Γ^q	Boundary on which heat flux q* is specified
Γ^t	Boundary on which traction t* is specified
Γ^u	Boundary on which velocity u* is specified
Δt	time increment
θ	time step factor
λ	Penalty coefficient (usually $10^7\mu$)
μ	Newtonian viscosity
ρ	Density
τ	Deviatoric stress tensor
Ω	Problem domain (volume, area, etc.)
∇	Laplacian operator

ACKNOWLEDGEMENTS

The authors gratefully acknowledge the support of this work by the Army Materials and Mechanics Research Center, the National Aeronautics and Space Administration through MIT's Materials Processing Center, and the Hysol-Dexter Corp.

REFERENCES

1. Zienkiewicz, O.C. "The Finite Element Method"; McGraw-Hill: London, 1977.

2. Hughes, T.R.J., Liu, W.K., and Brooks, A.J., J. Comp. Physics, 30, 1-60, 1979.

3. Gresho, P.M., and Lee, R.L., Computer and Fluids, 9, 223-253, 1981.

4. Roylance, D., "Finite Element Modeling of Nonisothermal Polymer Flows," Computer Application in Coatings and Plastics, ACS Symposium Series, in press.

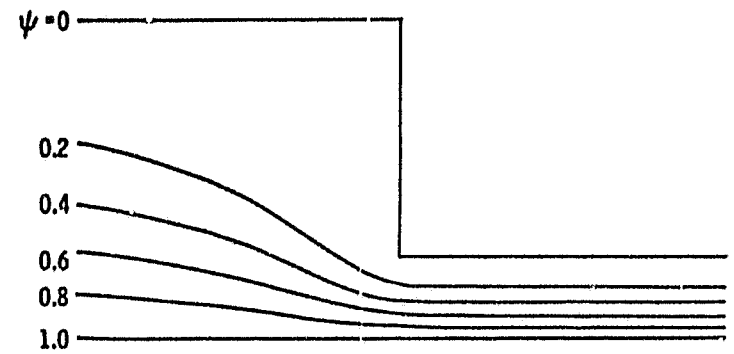

Figure 1 - Streamlines for 4:1 Newtonian entry flow.

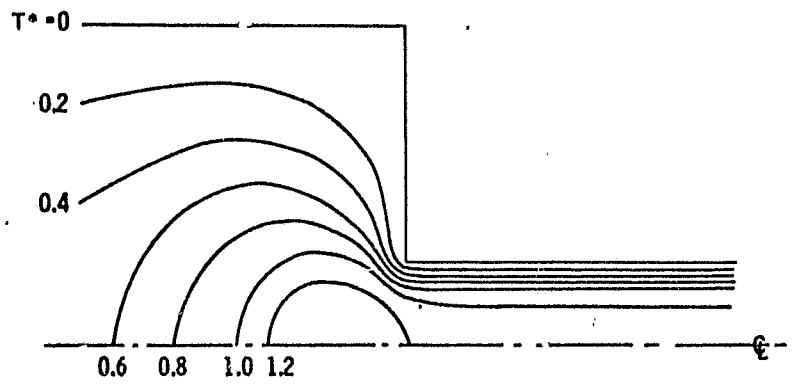

Figure 2 - Normalized temperature contours for 4:1 entry flow, Pe = 0.

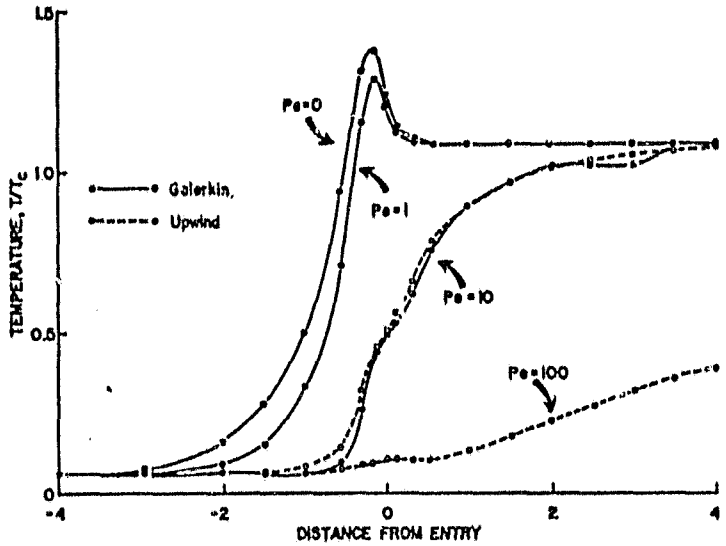

Figure 3 - Centerline temperatures in 4:1 entry flow, at various Peclet numbers.

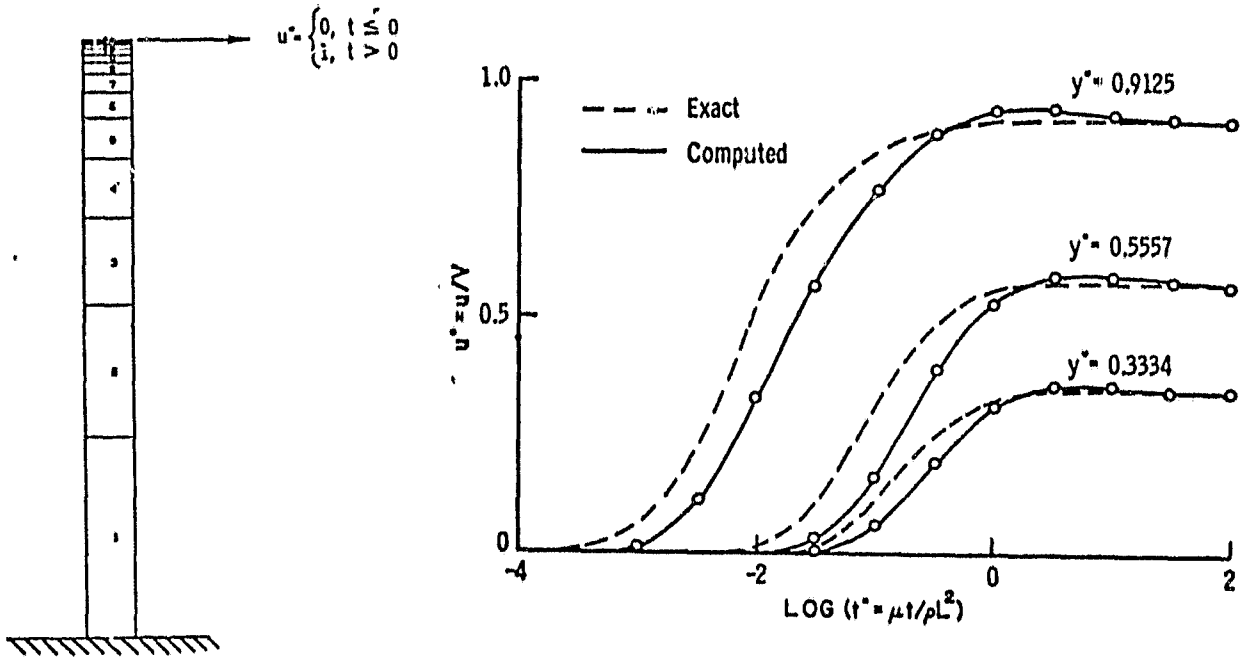

Figure 4 - Transient Couette flow - grid and velocity histories at various stations.

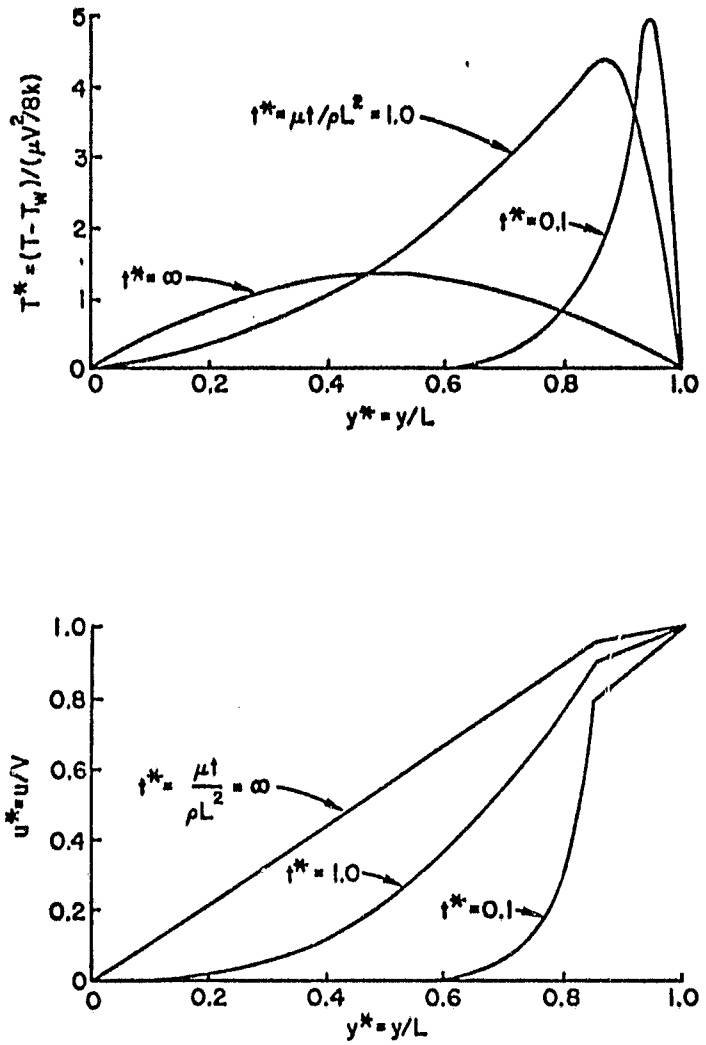

Figure 5 - Transient Couette flow of stratified immiscible fluids - temperature and velocity profiles at various times.

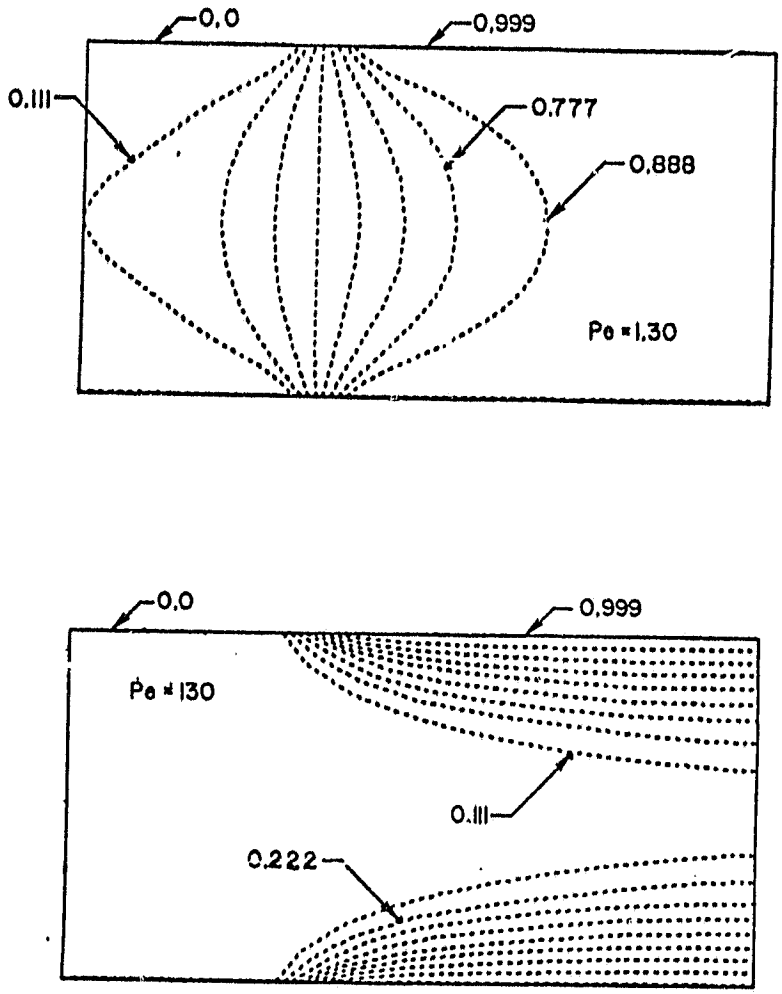

Figure 6 - Isothermal contours for Graetz flow at two Peclet numbers. Transition from cool to heated boundary is spread over one element width.